Homework 3 Write Up

Jalyn-Rose Clark

October 28, 2024

1 Oscillatory Motion and Chaos

1.1 Analytical calculation at what value Ω_D the resonance occurs

The equation of motion for the undamped, damped, and driven pendulum is defined by the differential equation:

$$\frac{\mathrm{d}^2\theta}{\mathrm{d}t^2} = -\frac{g}{l}\theta - 2\gamma\frac{\mathrm{d}\theta}{\mathrm{d}t} + \alpha_{\mathrm{D}}\sin(\Omega_D t) \tag{1}$$

For the driven pendulum, we can use the steady-state solution:

$$\theta(t) = \theta_0\sin(\Omega_D t + \phi) \tag{2}$$

The amplitude of the driven oscillator is:

$$\theta_0 = \frac{\alpha_{\mathrm{D}}}{\sqrt{(\omega_0^2 - \Omega_{\mathrm{D}}^2)^2 + (q\Omega_{\mathrm{D}})^2}} \tag{3}$$

The frequency at which resonance occurs will be at the maximum of the amplitude. The denominator of the amplitude function is differentiated with respect to Ω_{D} and then set equal to 0.

$$\frac{\mathrm{d}}{\mathrm{d}\Omega_{\mathrm{D}}}\left[(\omega_0^2 - \Omega_{\mathrm{D}}^2)^2 + (q\Omega_{\mathrm{D}})^2\right] \tag{4}$$

$$4\Omega_{\mathrm{D}}^3 - 4\omega_0^2\Omega_{\mathrm{D}} + 8\gamma^3\Omega_{\mathrm{D}} = 0 \tag{5}$$

$$\Omega_{\mathrm{D}} = 0 \tag{6}$$

$$\Omega_{\mathrm{D}} = -\sqrt{\omega_0^2 - 2\gamma^2} \tag{7}$$

$$\boxed{\Omega_{\mathrm{D}} = \sqrt{\omega_0^2 - 2\gamma^2}} \tag{8}$$

Using our given parameters, we can calculate the angular frequency at which resonance occurs in the driven case.

$$\Omega_{\mathrm{D}} = \sqrt{(\frac{9.8\frac{\mathrm{m}}{\mathrm{s}^2}}{9.8\mathrm{m}})^2 - 2(0.25\mathrm{s}^-1)^2} \tag{9}$$

$$\Omega_{\mathrm{D}} \approx 0.9354... \ \frac{\mathrm{rad}}{\mathrm{s}} \tag{10}$$

I expect the small angle approximation to be good because the α_{D} is small, so the driving force is weak, meaning θ will be small throughout the motion. This could also be determined by the initial angle, which isn't given to us, but I will use 15 degrees.

1.2 Numerical Solutions for Linear Oscillation

1.2.1 Linear oscillatory motion

Numerically, simple linear non-damped harmonic motion was solved using Euler-Cromer method.

$$\omega_{i+1} = \omega_i - \frac{g}{l}\theta_i\Delta t \tag{11}$$

$$\theta_{i+1} = \theta_i + \omega_{i+1}\Delta t \tag{12}$$

$$t_{i+1} = t_i + \Delta t \tag{13}$$

1.2.2 Damped oscillatory motion

For a pendulum with dissipation numerically the Euler-Cromer method is used where the pendulum is either underdamped, overdamped, or critically damped depending on the parameters.

$$\omega_{i+1} = \omega_i - \frac{g}{l}\theta_i \Delta t + q\omega_i \Delta t \tag{14}$$

$$\theta_{i+1} = \theta_i + \omega_{i+1}\Delta t \tag{15}$$

$$t_{i+1} = t_i + \Delta t \tag{16}$$

1.2.3 Driven pendulum oscillatory motion

For the driven pendulum, Runge-Kutta 4th Order is used.

$$k1_\omega = \Delta t(-\frac{g}{l})\theta - 2\gamma\omega + \alpha sin(\omega_D t) \tag{17}$$

$$k1_\theta = \Delta t\omega \tag{18}$$

$$k2_\omega = \Delta t - (\frac{g}{l})(\theta + \frac{k1_\theta}{2}) - 2\gamma(\omega + \frac{k1_\omega}{2}) + \alpha sin(\omega_D t + \frac{\Delta t}{2}) \tag{19}$$

$$k2_\theta = \Delta t(\omega + \frac{k1_\omega}{2}) \tag{20}$$

$$k3_\omega = \Delta t - (\frac{g}{l})(\theta + \frac{k2_\theta}{2}) - 2\gamma(\omega + \frac{k2_\omega}{2}) + \alpha sin(\omega_D t + \frac{\Delta t}{2}) \tag{21}$$

$$k3_\theta = \Delta t(\omega + \frac{k2_\omega}{2}) \tag{22}$$

$$k4_\omega = \Delta t - (\frac{g}{l})(\theta + \frac{k3_\theta}{2}) - 2\gamma(\omega + \frac{k3_\omega}{2}) + \alpha sin(\omega_D t + \frac{\Delta t}{2}) \tag{23}$$

$$k4_\theta = \Delta t(\omega + k3_\omega) \tag{24}$$

$$\omega[i+1] = \omega + \frac{1}{6}\Big(k1_\omega + 2k2_\omega + 2k3_\omega + k4_\omega\Big) \tag{25}$$

$$\theta[i+1] = \theta + \frac{1}{6}\Big(k1_\theta + 2k2_\theta + 2k3_\theta + k4_\theta\Big) \tag{26}$$

1.2.4 $\theta(t)$ and $\omega(t) = \frac{d\theta}{dt}$

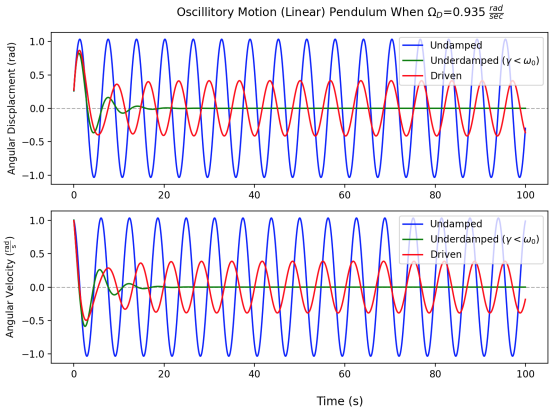

Figure 1: Comparison of Undamped, Underdamped, and Driven Linear Pendulum

1.2.5 Mapping out the resonance structure $\theta_0(\omega_D)$ and $\phi(\omega_D)$

The FWHM of resonance was extracted to be **13.73641347**.

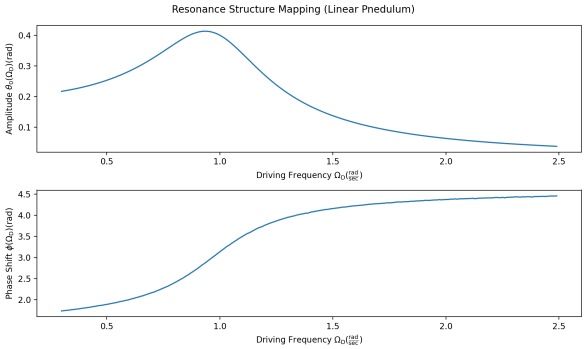

Figure 2: Amplitude and Phase Shift for Different Driving Frequencies

1.3 Energy of the pendulum

At a **driving frequency of 0.935** (close to resonance), potential, kinetic, and total energies were plotted over circa 10 periods.

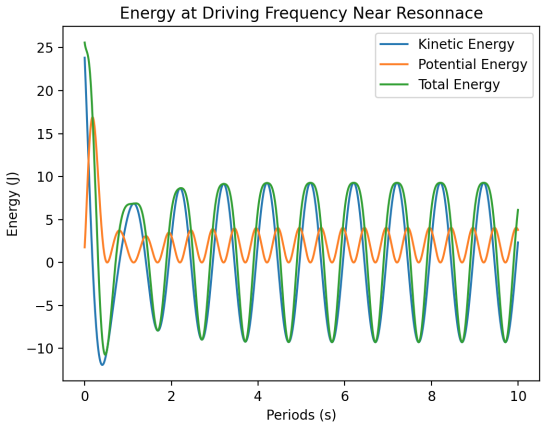

1.4 Non-Linear Effects

The non-linear pendulum was plotted at a frequency close to resonance, **driving frequency of 0.935** and right above resonance **driving frequency of 1.2** and compared to the linear pendulum motion. (Fig. 3) The difference in the curve between the two driving frequencies is very small, but there is a subtle difference between the Non-Linear and the Linear pendulum. I used an angle of **15 radians**, the small angle approximation held true.

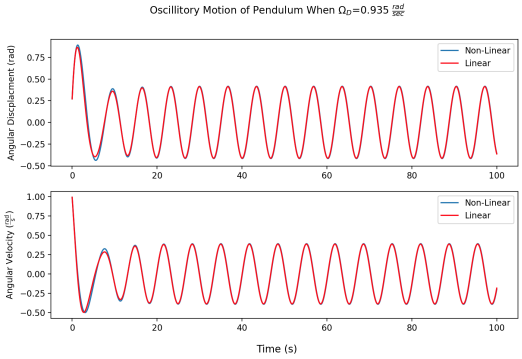

Figure 3: At a driving frequency close to resonance $\mathbf{0.935\frac{rad}{sec^2}}$

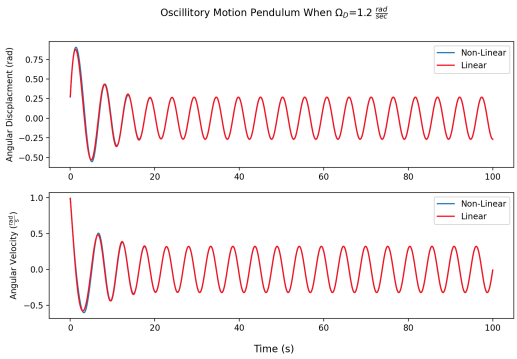

Figure 4: At a driving frequency above resonance $\mathbf{1.2}\,\mathbf{\frac{rad}{sec^2}}$

1.5 Lyapunov exponent of the system

The non-linear pendulum was used to compute $\Delta\theta(t)$ for several trajectories with slightly different initial angles. (Fig. 4)
System 1 $\alpha_\mathbf{D} = \mathbf{0.2} :\rightarrow \lambda = -0.24$
System 2 $\alpha_\mathbf{D} = \mathbf{0.5} :\rightarrow \lambda = -0.23$
System 3 $\alpha_\mathbf{D} = \mathbf{01.2} :\rightarrow \lambda = -0.07$

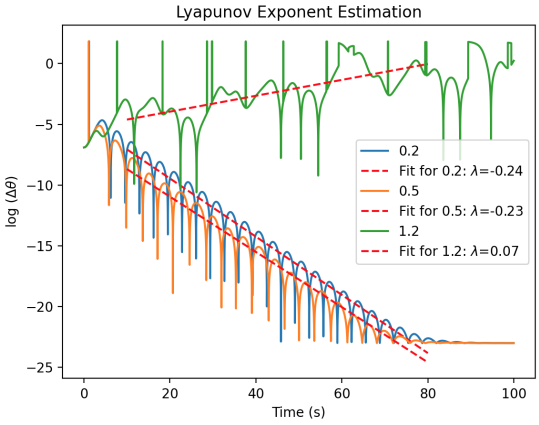

Figure 5: Numerical Data for Lyapunov exponent and fit.

A Lyapunov exponent less than 0 agrees with a nonchaotic system where the system is not sensitive to initial conditions. A Lyapunov exponent greater than 0 agrees with a chaotic system where the system's behavior becomes unpredictable and is sensitive to initial conditions.

2 Poisson Equation for Dipole

2.1 Solving Poisson's equation

Solving Poisson's equation gives us the regions with charge density (ρ) at our dipole locations. With ∇^2 being the Laplace operator, V being the electric potential, and ϵ_0 being the permittivity of free space.

$$\nabla^2 V = \frac{\rho}{\epsilon_0} \tag{27}$$

On our grid, we can assign two point charges, +q and -q, representing the dipole's negative and positive charges. Where the charge density is 0 ($\rho = 0$) far away from the dipole, we can simplify Poisson's equation from our dipole to the Laplace equation.

$$\nabla^2 V = 0 \tag{28}$$

Using the provided methods, we can calculate the electric potential of the static electric dipole by using the solved Poisson equation in Cartesian coordinates with a spherical boundary, $V(R) = 0$.

2.2 Gauss-Seidel algorithm for conformation

The Gauss-Seidel algorithm was first used to confirm the calculations because it converges faster and uses less memory, and new values are used as soon as they are available. In a 2D grid using Cartesian coordinates, the V is updated using the equation.

$$V_{new}(i,j) = \frac{1}{4}\Big(V_{old}(i+1,j) + V_{new}(i-1,j) + V_{old}(i,j+1) + V_{new}(i,j-1)\Big) \tag{29}$$

At the grid points, when the charge density is not 0 (at the dipole points), the algorithm equation can be modified.

$$V_{new}(i,j) = \frac{1}{4}\Big(\text{“”}\Big) + \frac{\rho(i,j)\Delta x^2}{\epsilon_0} \tag{30}$$

2.3 Jacobi Relaxation algorithm

The Jacobi relaxation method uses old values from the previous iteration and waits until the full grid is updated, causing it to have a slower convergence.

$$V_{new}(i,j) = \frac{1}{4}\Big(V_{old}(i+1,j) + V_{old}(i-1,j) + V_{old}(i,j+1) + V_{old}(i,j-1)\Big) \tag{31}$$

At the grid points, when the charge density is not 0 (at the dipole points), the algorithm equation can be modified.

$$V_{new}(i,j) = \frac{1}{4}\Big(\text{“”}\Big) + \frac{\rho(i,j)\Delta x^2}{\epsilon_0} \tag{32}$$

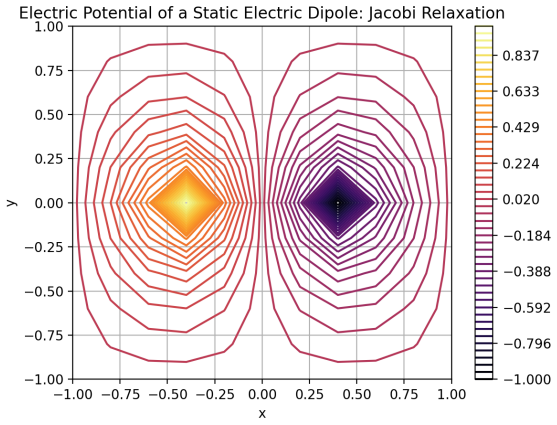

Figure 6: Equipotential lines of electric potential of a static electric dipole with the color bar representing V.

Accoriding to large-distance behavior of the dipole potential, the potential of an electric dipole decreases proportionally to $\frac{1}{r^2}$

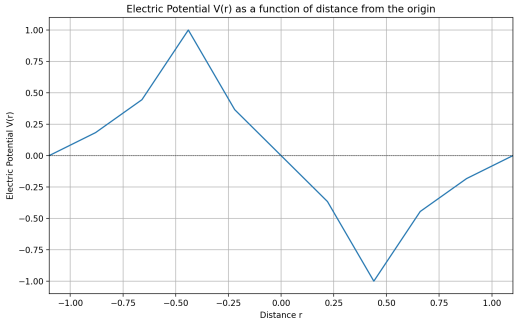

Figure 7: V(r) (r is the distance from the origin)

2.4 Relationship between $N_{\mathbf{iter}}$ and ϵ

The number of required iteration steps increases with the reduction of the tolerance is what is expected.(Fig. 8)

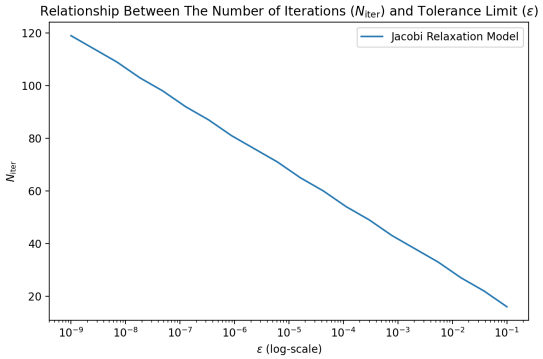

Figure 8: Decreasing tolerance limit with increasing iterations.

2.5 Simultaneous Over Relaxation Method

The Simultaneous over relaxation method is similar to Jacobi but it converges faster and accuracy is be defined as largest relative change of a single gridpoint from one iteration to the next. The relationship between the number of iteration steps and the grid size was investigated. **I found that $\mathbf{N_{iter} \propto L^2}$ for Jacobi and $\mathbf{N_{iter} \propto L}$ for the simultaneous over relaxation.**

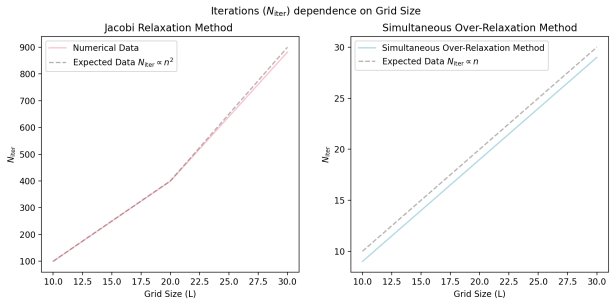

Figure 9: Relationship between the number of iteration steps and the grid size.